

Growth, Single-Crystalline Rutile TiO₂ Nanorod Thin Film By Hydrothermal Technique

¹Zuhair H. Nasser

²Sattar J. Kasim

³Whidad S. Hanoosh

¹Southern Technical University, Technical Institute of Basrah.

²Basrah university, College of Science, Dep. of Phys.

³Basrah University, College of Science, Dep. of Chem.

*Corresponding author E-mail: zuhhsh@stu.edu.iq

KEYWORDS :

- Hydrothermal technique
- growth single-crystalline rutile TiO₂ nanorod thin films

ABSTRACT

A facile, hydrothermal technique was developed to growth, single-crystalline rutile TiO₂ nanorod thin films on transparent conductive fluorine-doped tin oxide (FTO) substrates. In this study, the deferent periods(6, 9, 12, 15, and 18 hour) were selective with constant temperature at 160 °C to growth this films and growth in deferent temperature (130, 150,170,190, and 210 °C) with constant period of deposition at 6h. SEM image showed all the films were nanorodand the EDX measurement was given the portion of element that contribution in rutile TiO₂ nanorod thin films. The diameter, length, and density of the nanorods could be varied by changingthe growth parameters. The XRD to determine the structure properties, and optical properties were measured of these rutile TiO₂ nanorod thin films and obtained the absorbance and energy gap.

<http://dx.doi.org/10.31257/2018/JKP/100206>

تطوير تقنية الأنماء للأغشية الرقيقة ذات القضبان النانوية أحادية التبلور لمركب ثنائي أكسيد التيتانيوم تركيب الروتايل

^٣وداد صالح حنوش

^٢ستار جبار قاسم

^١زهير هشام ناصر

^١الجامعة التقنية الجنوبية، المعهد التقني /بصرة.
^٢جامعة البصرة، كلية العلوم، قسم الفيزياء
^٣جامعة البصرة، كلية العلوم، قسم الكيمياء

الكلمات المفتاحية:

- تقنية التحلل الحراري
- انماء بلورة TiO₂ احادية التبلور
- أغشية قضبان نانوية رقيقة

الخلاصة

لقد تم تطوير تقنية الأنماء للأغشية الرقيقة ذات القضبان النانوية أحادية التبلور لمركب ثنائي أكسيد التيتانيوم تركيب الروتايل على قواعد زجاجية مطلية بطبقة شفافة و موصلة من (FTO).و ذلك بانتقاء فترات ترسيب مختلفة (6, 9, 12, 15, and 18 hour) بثبوت درجة الحرارة عند 160°C ودرجات حرارية مختلفة (130, 150,170,190, 210 °C) بثبوت فترة الترسيب 6h. تم قياس الخواص التركيبية عن طريق الصور الملتقطة بواسطة جهاز المجهر الإلكتروني الماسح وقياسات (EDX) إضافة الى قياسات (XRD) وأظهرت أن الأغشية الرقيقة تعود الى TiO₂ ذات قضبان بقياسات نانوية . وقد تم حساب أقطار وكثافة القضبان النانوية. كما أجريت القياسات على الأغشية لتحديد خواصها البصرية يثبت تم تحديد حافة و معامل الامتصاص إضافة الى فجوة الطاقة البصرية.

1. Introduction

Titanium dioxide discovered in 1821, {Formatting Citation} is occupied one of the top 20 inorganic chemicals of industrial importance. The compound used in the commercial manufacture began around 1916, then development of investigation has been got increases since that time.[1-3]

Titania nano particles have received much interest for applications such as optical devices, sensors, and solar cell applications. There are several factors in determining important properties in the performance of TiO₂ for applications such as particle size, crystallinity and the morphology. [5-6]

Titanium dioxide has been derived from element or other titanium molecules and cannot occur pour in nature. When TiO₂ is irradiated by photons with an energy higher than or equal to its band gap (~3.2 eV), through photon absorption, the electrons can be promoted to the conduction band, generating holes in the valence band.

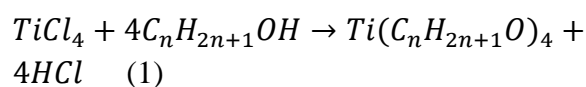
Titanium-di-oxide is the most attracted materials in nanoscience and nanotechnology because of having a lot of interesting properties from fundamental and practical point of view. [1].

TiO₂ is a commonly used semiconductor for photon-electron transfer processes. Several methods for the preparation of Nano crystalline TiO₂ have been developed and they are electrochemical reaction, continuous reaction, supercritical carbon dioxide, precipitation, multi-gelation, chemical solvent and chemical vapor decomposition, ultrasonic irradiation, RF sputtering, sol-gel, Aerogel, Xerogel [1- 25] and hydrothermal method.[1, 3], [26-30]

2. Experimental part:

In our present work precursor of titanium butoxide (TTB) were used to growth rutile nanorod titanium dioxide thin film The precursor prepared as following way: Three

neck container (250ml) and separation final (50 ml) were carefully cleaned and sit to the holder. We take equivalent weight according to the equation (1) from Titanium tetrachloride (TiCl₄) and butanol.



$$w_{Co} = \frac{w_{TiCl_4} \times 4Mw_{Co}}{Mw_{TiCl_4}} \quad (2)$$

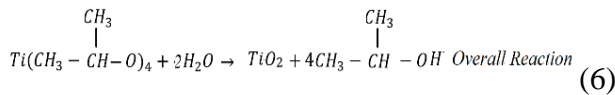
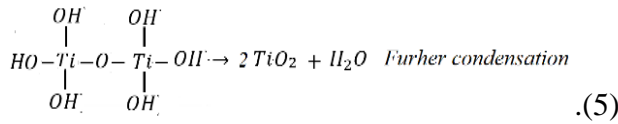
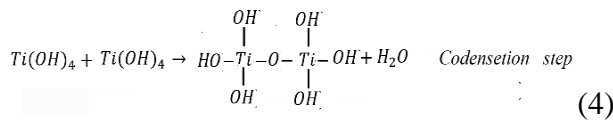
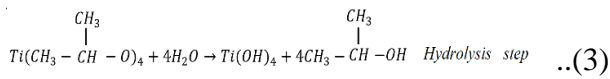
Where Mw_{Co} & Mw_{TiCl_4} are the molecular weight of alcohol and Titanium tetrachloride respectively, and w_{Co} & w_{TiCl_4} are the weight of alcohol and Titanium tetrachloride respectively.

Put the amount of the Titanium tetrachloride in the three-neck container (250ml) and stirring, (TiCl₄ is a compound with strong ability to absorb the H₂O to make heavy fog). Thus, governs the closure of two necks, the other neck is leave to separation final tube to dropped into 3-neck container. Leave the separation final slowly dropped until the fog is perfectly vanish. In this reaction the band between titanium and chlorine is broken and new band is formed between titanium and tetra-butoxide, after the n-butanol losses the hydrogen ion to the chlorine ion to formed 4HCl.

Hydrothermal method:

When the substrate of glass coating F:SnO₂ be ready, we put it in the Teflon-lined stainless steel autoclave container (is washing in distilled water and ethanol carefully and dried in the oven for 15 minutes) with angle where the conducting side facing up. The precursor was prepared by mixed 15ml of deionized water with 15ml of HCl and stirring for 15 minute before added 0.5ml of (TTB) and leave on stirring for 5 minute. Then, we put into the Teflon governs the closure and put in the oven.

The chemical reaction acted as following equations:



In this study, we take temperature at 160 °C different time periods 3, 6, 9, 12,15and18 hours

3. Results and discussion:

(SEM) image: effected of the time:

Nanorod thin film of titanium dioxide had been synthesised by using hydrothermal method with variation of the time of deposition and fixed temperature at 160°C.

Table (1): values of length and diameter of the nanorod.

sample	period of deposition h	Temp. of deposition °C	Rate length of rod μm	Rate diameter of rod nm	spate ratio
p1	6	160	1.70	79	22
p2	9	160	3.50	103	32
p3	12	160	6.00	113	53
p4	15	160	7.00	114	61
p5	18	160	6.63	113	58

The deposition for 3h the rods did not grow, thus, (SEM) image does not exist. In figure (1a) illustrate surface of nanorod thin film deposited at various periods, the right of length of the nanorods can be seen increase when the period of deposition increases, while right of diameter started with clear increases, then had less difference for longer periods.

Ratio of nanorods' number with respect to diameter in SEM images of single-crystalline rutile TiO₂ nanorod thin films growth at (150,

170, 190 and 210 °C) for 12 h were growth on the (FTO) layer.

The top surfaces of all rods are square or rectangle. Each rod seemed as gathered many nanorod. The effect of time growth is explained on the length of the rod. The surface image illustrated the homogenous in area of a rods' surface, and the greatest number of the rods are in nanoscale as seen in figure (1).The ratio length/diameter of nanorods increase with respected to period of deposition for the sample P1, P2, and P3 then fixed of other sample as seen in figure (2).

Effected of the time:

Single-crystalline rutile TiO₂ nanorod thin films growth at (130, 150, 160, 170, 180,190 and 210 °C) for 12 h were growth on the (FTO) layer. When deposition at 130 °C the rods are not growth, thus, (SEM) image do not exist. The image of (SEM) as in figure (3a) is illustrate surface of nanorod thin film deposited at 150°C the greatest of rutile nanorods lays under 100nm

because the nanorod had been deposited in slow mechanism it can be seen in more regular future. The man diameter of the nanorods were 75nm. In figure (1c) is illustrate surface of nanorod thin film deposited at 160 °C we see that in previos. In figure (3b) is illustrate surface of nanorod thin film deposited at 170 °C,the mean diameter 150nm. In figure (3c) is illustrate surface of nanorod thin film deposited at 190 °C, the mean diameter 150nm. In figure (3d) is illustrate surface of nanorod thin film deposited at 210 °C, the man diameter 170nm. This nanorod thin film was dislocated the FTO layer with film from the glass substrate.

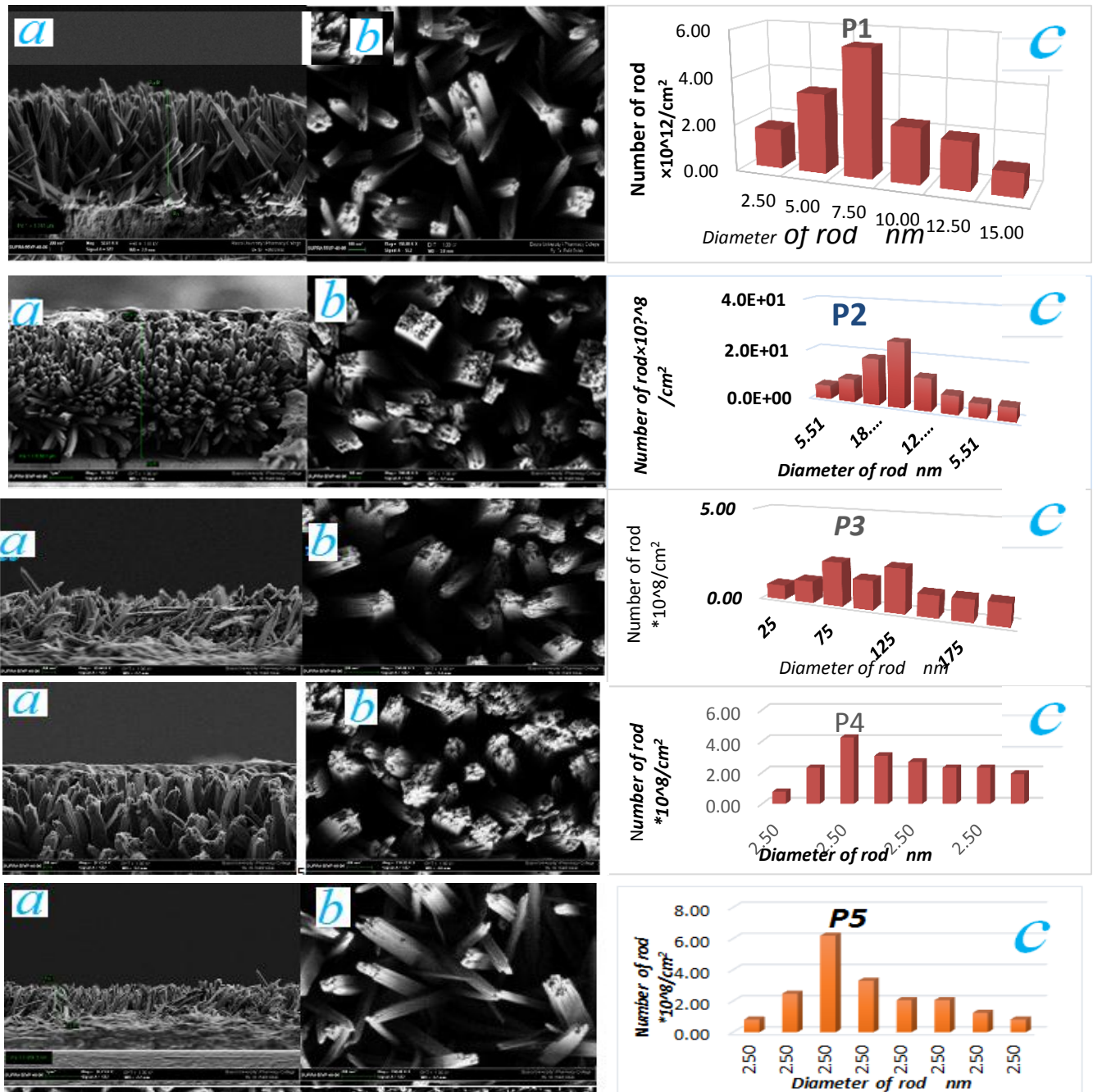


Figure (1): Illustrate surface, Cross section and the ratio of nanorods' number with respect to diameter in SEM images of single-crystalline rutile TiO₂ nanorod thin films growth for (6, 9,12,15,and 18 h) at 160 °C were growth on the (FTO) layer.

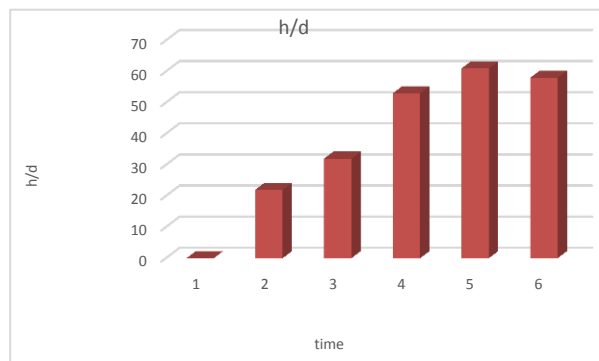


Figure (2): The diagrams of (a) the height/diameter of rods VS the period of deposition of single-crystallinerutile TiO₂ nanorod thin films.

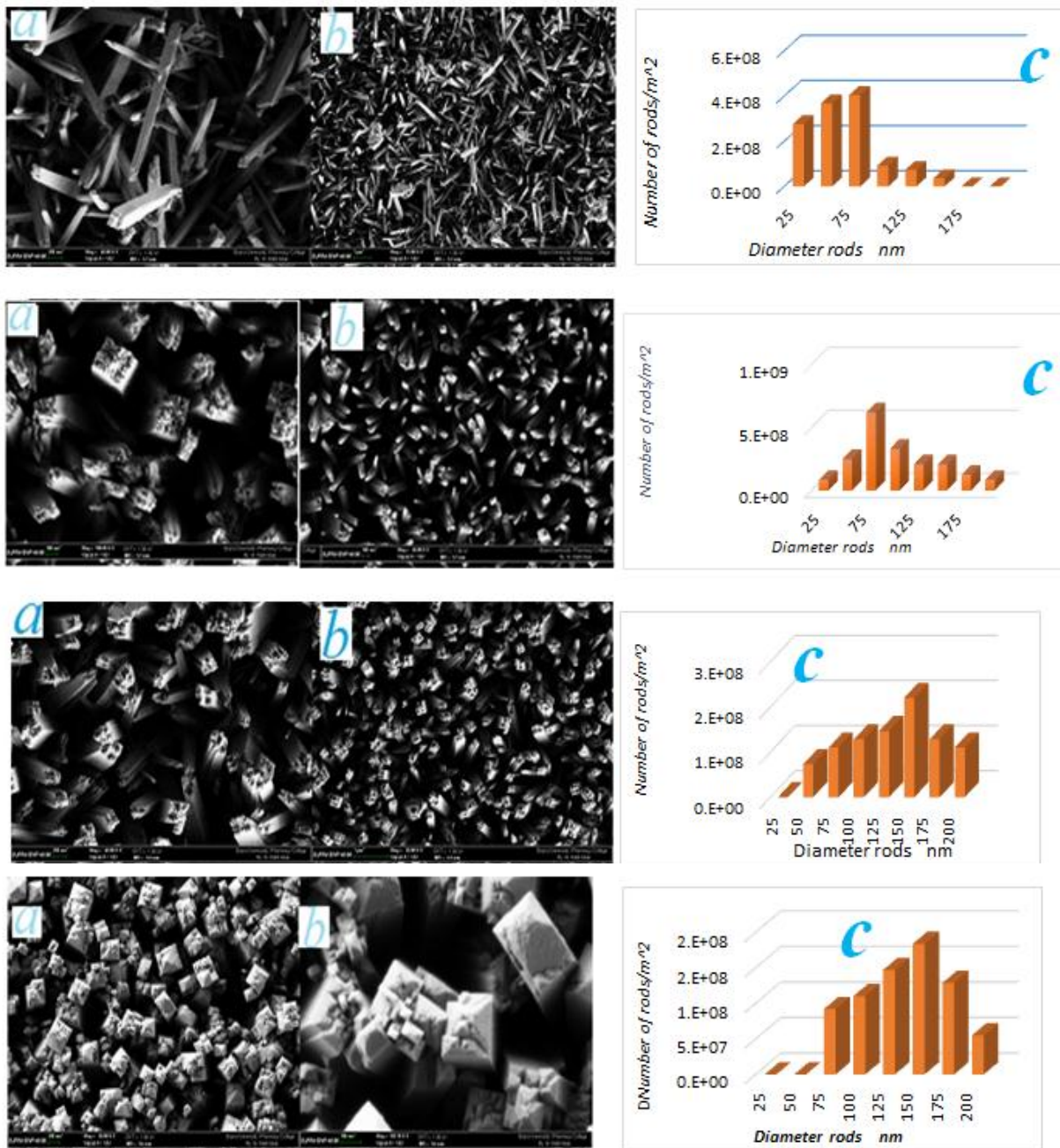


Figure (3): Illustrate surface, Cross section and the ratio of nanorods' number with respect to diameter in SEM images of single-crystalline rutile TiO₂ nanorod thin films growth at (150, 170, 190 and 210 °C) for 12 h.

Table (2) value of diameter of the nanorod.

sample	period of deposition h	Temp. of deposition °C	Rate diameter of rod nm
pt1	12	150	75
pt3	12	170	90
pt4	12	190	150
pt5	12	210	160

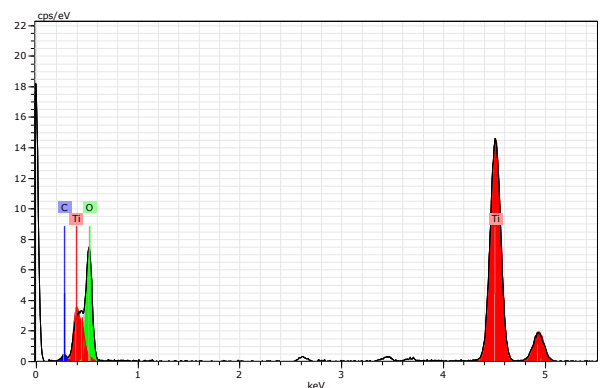


Figure (4): EDX chart of single-crystalline rutile TiO₂ nanorod thin films.

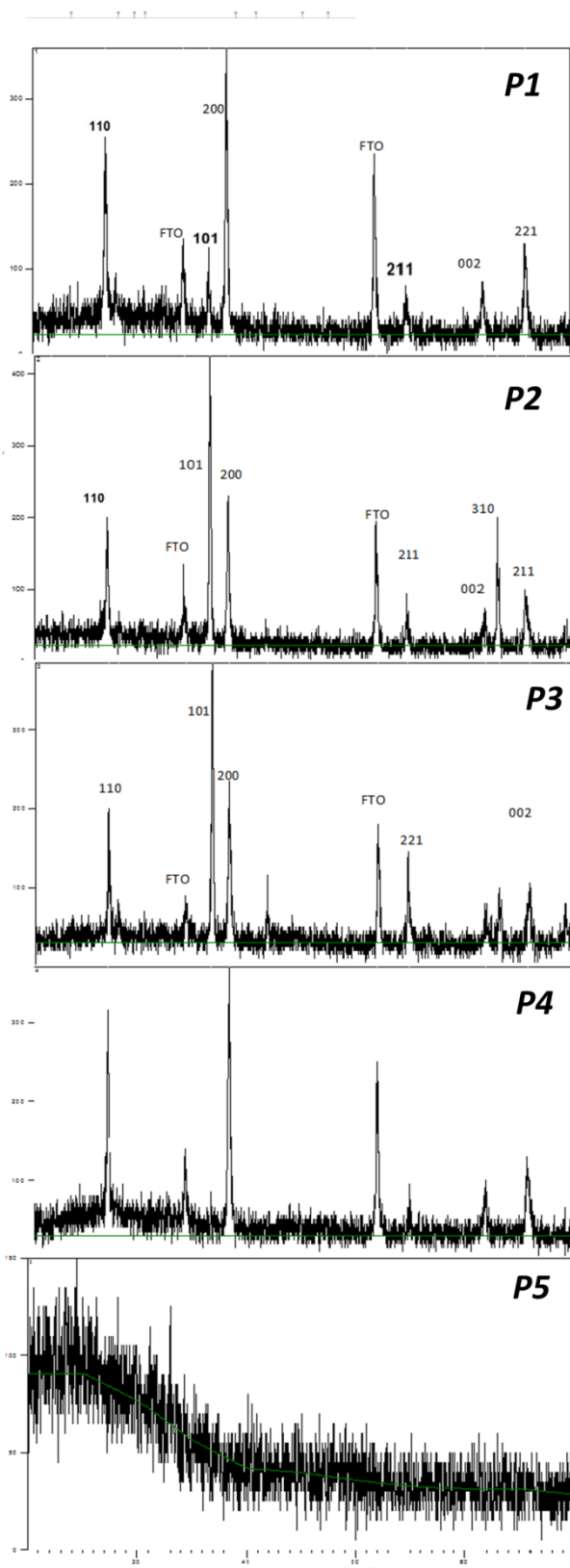


Figure (5): Charts of X-RAY diffraction Measurement of the thin films of titanium dioxide nanorod rutile thin films deposition for 6, 9, 12, 15, 18h at 160 °C.

The nanorod thin film has been composed essentially from Ti and O elements in ordinary portion, which include in the TiO₂ compound.

X-RAY Diffraction Measurement:

In the figure (5)) are for x-ray diffraction charts of single-crystalline rutile TiO₂ nanorod thin films deposited on the glasses substrate coated FTO using butoxide precursor for 6, 9, 12, 15, 18h periods of time respectively deposited at 160 oC. prepared TiO₂ nanorods are composed of a mainly tetragonal rutile phase (JCPDS No.: 860147, a=b= 4.594 °A, c = 2.958 °A)

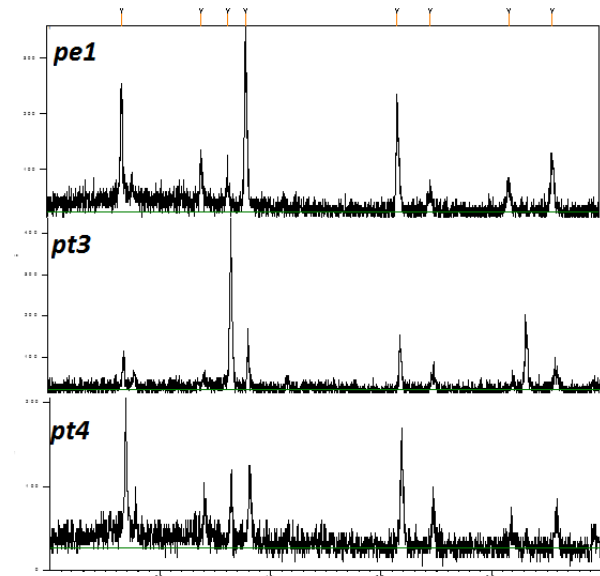


Figure (6): Charts of X-RAY diffraction Measurement of the thin films of titanium dioxide nanorod rutile thin films deposition at 150, 170, 190 °C for 12h.

In the figure (5a) the peak 2 thetas at 26.77, refer the thin film is rutile. The experimental of lattice constant (a=b= 4.722 Å and c= 2.838 Å).

In the figure (5b) the peak 2 theta at 26.77, refer the thin film is rutile. The experimental of lattice constant (a=b= 4.72 Å and c= 2.8410 Å). In the figure (5c) the peak 2 theta at 26.77, refer the thin film is rutile. The experimental of lattice constant (a=b= 4.7018 Å and c= 2.798Å). In the figure (5d) the peak 2 theta at 26.77, refer the thin film is rutile. The experimental of lattice constant (a=b= 4.7185 Å and c= 2.8330Å). The last nanorod thin film where growth for 18 h at 160 °C shown in Figure (5e) seems have no peaks because the result of increases of rods' lengths leads to

broken this rods then full the area between the rods that's due unregimented in the structure when we compared with the other nanorod thin film. The greatest structure growth for the nanorod thin film when we growth for 6 and 15h in (200) direction, while that growth for 9 and 12h in (101) direction that's agree with[31]. This variation is due to deference in the size of the nanod of the thin films.

In the figures (6) x-ray diffraction charts of single-crystalline rutile TiO₂ nanorod thin films deposited on the glasses substrate coated FTO using butoxide precursor for 150, 170, and190 °C respectively deposited at 12h. All films are in rutile structure a bare from the peak at the 2 theta 26.77° as we illustrated in above section. In addition, the peak at 2 theta 63.07 was grown in the figures (6). There are no clear peak belong to the TiO₂ for thin film grown at 210 °C because the arise in temperature causes rapid growth and therefore leads to irregularity in crystalline construction

Optical properties:

The optical properties of this samples obtained by Shmadzu 1800 UV-Vis spectroscopy, where absorbance measurements. The figure (7a) illustrate the absorbance as function to the wavelength for the setoff nanorod thin films growth at 160 °C for different period. A variety can be seen in the absorbance of each sample with according to the thickness crystallinity to the structure of nanorod thin films . the absorption edge is go to the short wavelength when the period of time increase. The figure (7b) illustrate the Absorption Coefficientto the photon energy by using the lambert beer law eq.(7) and (8)

$$\frac{I}{I_0} = e^{-\alpha z} \dots \dots \dots (7)$$

where (α) and (z) are the absorption coefficient thickness of the sample by solve this equation with the absorbance we get:

$$\alpha = \frac{2.303A}{z} \dots \dots \dots (8)$$

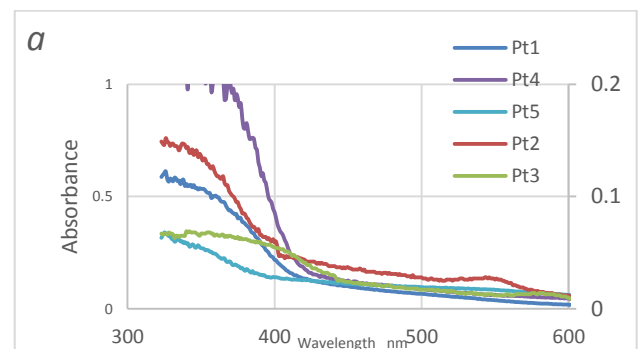
Reason wherever got increases in the thickness can be followed increases absorption coefficient. From the figure (7c) it can predicts with the absorption edge then the optical energy gap can determine. In figure (7e) the optical energy gap was calculated using the relation:

$$\alpha h\nu = A_o (h\nu - E_g)^n \dots \dots \dots (9)$$

It can be seen in the figure (7.b) the absorption coefficient increases with increase of thickness. That is ordinary, where hv is the photon energy, A_o the constant associated with ordered crystalline structure, and n the exponent depending on the type of optical transitions is equal to ½ for indirect gap and 2 for direct gap.

There is a simple deference in the value of energy gap that is came from deference in the nanorod size. The increase in crystallization and regularity in the crystalline construction of the thin film may be also as a reason. From the figure (7) the five curve are nanorod TiO₂ thin films, the sample (p1) illustrated the absorption properties. All the curves have great value of absorbance near IR region. Then the decreases between (370-480 nm) where the titanium dioxide have high value of transmittance in the visible region of the electromagnetic spectrum. The smooth surface and the nano size of rods are act to decreases of the absorption coefficient. The fundamental absorption edge lays between (370-450 nm).

The energy gap is about 2.8-3.2 eV. This variation is due to deference in the size of the nanorod of the thin films according to increase of the period and temperature of deposition.



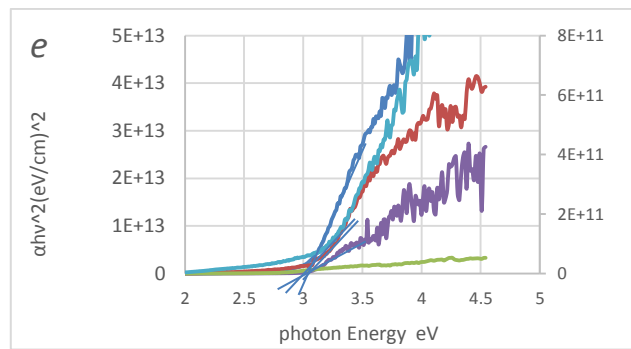
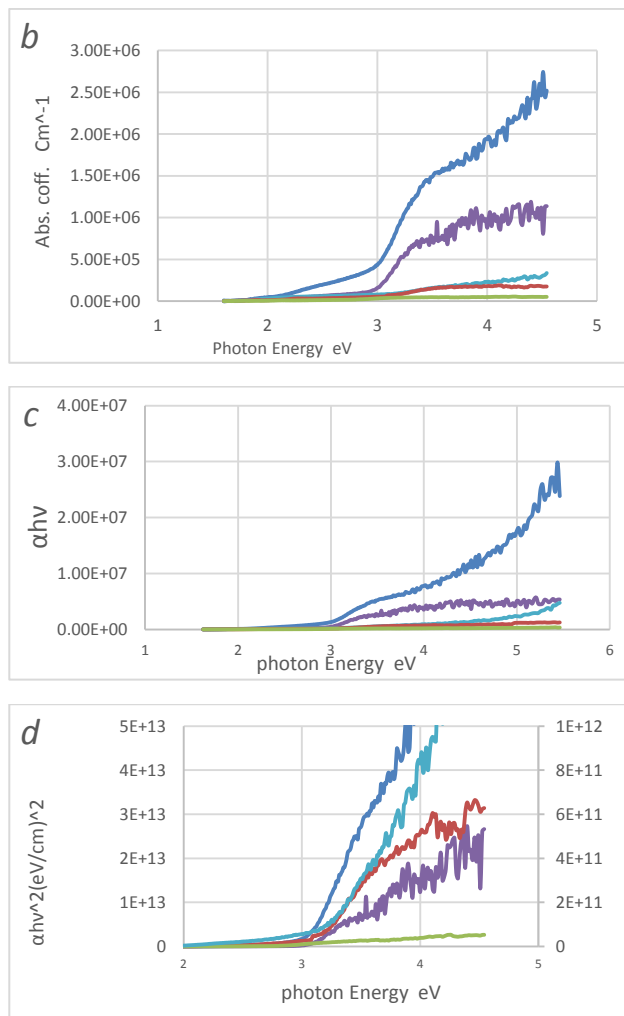


Figure (7): illustrate the optical properties of single-crystalline rutile TiO_2 nanorod.

- [1] Anodization Methods,” *Optoelectron. - Adv. Mater. Devices*, pp. 115–136, 2013.
- [2] S. Ito et al., “Fabrication of thin film dye sensitized solar cells with solar to electric power conversion efficiency over 10%,” *Thin Solid Films*, vol. 516, no. 14, pp. 4613–4619, 2008.
- [3] S. Lattante, “Electron and Hole Transport Layers: Their Use in Inverted Bulk Heterojunction Polymer Solar Cells,” *Electronics*, vol. 3, no. 1, pp. 132–164, 2014.
- [4] R. Richards and F. Group, *S URFACE AND N ANOMOLECULAR* edited by. 2006.
- [5] A. Tohara, Y. Sugawara, and M. Sato, “Preparation and characterization of,” *J. Porphyr. Phthalocyanines*, pp. 104–116, 2006.
- [6] R. Liu, W. Yang, and H. Tsai, “Preparation and Visible-light Photocatalytic Activity of $\text{Pt/TiO}_2\text{-xNy}$,” *Emcs 2015*, no. Emcs, pp. 127–130, 2015.
- [7] S. Shironita and T. Takasaki, “Equilibrium state of anatase to rutile transformation for nano-structured Titanium Dioxide powder using polymer template method .”
- [8] H. Eslami, F. Moztarzadeh, T. S. J. Kashi, K. Khoshroo, and M. Tahriri, “Hydrothermal Synthesis and Characterization of TiO_2 -Derived Nanotubes for Biomedical Applications,” *Synth. React. Inorganic, Met. Nano-Metal Chem.*, vol. 46, no. 8, pp. 1149–1156, 2016.
- [9] D. Dissertation, “A Dual-Stage Hydrothermal Flow Reactor for Green and Sustainable Synthesis of Advanced Hybrid Nanomaterials,” 2016.
- [10] P. Pori et al., “Structural studies of TiO_2 /wood coatings prepared by hydrothermal deposition of rutile particles

- from TiCl_4 aqueous solutions on spruce (Picea Abies) wood,” *Appl. Surf. Sci.*, vol. 372, pp. 125–138, 2016.
- [11] H. Mehranpour, M. Askari, and M. S. Ghamsari, “Nucleation and Growth of TiO_2 Nanoparticles,” *Nanomaterials*, 2010.
- [12] M. E. El-Naggar, T. I. Shaheen, S. Zaghoul, M. H. El-Rafie, and A. Hebeish, “Antibacterial Activities and UV Protection of the in Situ Synthesized Titanium Oxide Nanoparticles on Cotton Fabrics,” *Ind. Eng. Chem. Res.*, vol. 55, no. 10, pp. 2661–2668, 2016.
- [13] S. Winkler, “Photoelectron Spectroscopy of Polarons in Molecular Semiconductors.”
- [14] R. Liu, “Hybrid organic/inorganic nanocomposites for photovoltaic cells,” *Materials (Basel)*, vol. 7, no. 4, pp. 2747–2771, 2014.
- [15] W. Li and T. Zeng, “Preparation of TiO_2 anatase nanocrystals by TiCl_4 hydrolysis with additive H_2SO_4 ,” *PLoS One*, vol. 6, no. 6, pp. 2–7, 2011.
- [16] T. Theivasanthi and M. Alagar, “Titanium dioxide (TiO_2) Nanoparticles XRD Analyses: An Insight,” *arXiv*, pp. 1307–1316, 2013.
- [17] X. Wang et al., “ TiO_2 nanotube arrays based flexible perovskite solar cells with transparent carbon nanotube electrode,” *Nano Energy*, vol. 11, pp. 728–735, 2015.
- [18] M. Sathish, B. Viswanathan, R. P. Viswanath, and C. S. Gopinath, “Synthesis, characterization, electronic structure, and photocatalytic activity of nitrogen-doped TiO_2 nanocatalyst,” *Chem. Mater.*, vol. 17, no. 25, pp. 6349–6353, 2005.
- [19] D. Emadzadeh et al., “Solvothermal synthesis of nanoporous TiO_2 : The impact on thin-film composite membranes for engineered osmosis application,” *Nanotechnology*, vol. 27, no. 34, p. 345702, 2016.
- [20] J. Pan, G. Liu, G. Q. Lu, and H. M. Cheng, “On the true photoreactivity order of {001}, {010}, and {101} facets of anatase TiO_2 crystals,” *Angew. Chemie - Int. Ed.*, vol. 50, no. 9, pp. 2133–2137, 2011.
- [21] B. Chen et al., “Graphene Oxide-Assisted Synthesis of Microsized Ultrathin Single-Crystalline Anatase TiO_2 Nanosheets and Their Application in Dye-Sensitized Solar Cells,” *ACS Appl. Mater. Interfaces*, vol. 8, no. 4, pp. 2495–2504, 2016.
- [22] S. K. Misra, S. I. Andronenko, D. Tipikin, J. H. Freed, V. Somani, and O. Prakash, “Study of paramagnetic defect centers in as-grown and annealed TiO_2 anatase and rutile nanoparticles by a variable-temperature X-band and high-frequency (236 GHz) EPR,” *J. Magn. Magn. Mater.*, vol. 401, pp. 495–505, 2016.
- [23] K. W. Böer, *Handbook of the Physics of Thin-Film Solar Cells*. 2013.
- [24] K. Thamaphat, P. Limsuwan, and B. Ngotawornchai, “Phase Characterization of TiO_2 Powder by XRD and TEM,” *Nat. Sci.*, vol. 42, pp. 357–361, 2008.
- [25] P. Roy, S. Berger, and P. Schmuki, “ TiO_2 nanotubes: Synthesis and applications,” *Angew. Chemie - Int. Ed.*, vol. 50, no. 13, pp. 2904–2939, 2011.
- [26] V. Tamilselvan, D. Yuvaraj, R. Rakesh Kumar, and K. Narasimha Rao, “Growth of rutile TiO_2 nanorods on TiO_2 seed layer deposited by electron beam evaporation,” *Appl. Surf. Sci.*, vol. 258, no. 10, pp. 4283–4287, 2012.
- [27] JAMIESON JC and OLINGER B, “Pressure-Temperature Studies of Anatase, Brookite Rutile, and TiO_2 (II). a Discussion,” *Am. Mineral.*, vol. 54, no. 9–10, pp. 1477–1481, 1969.
- [28] B. Liu and E. S. Aydil, “Growth of Oriented Single-Crystalline Rutile TiO_2 Nanorods on Transparent Conducting Substrates for Dye-Sensitized Solar Cells Growth of Oriented Single-Crystalline Rutile TiO_2 Nanorods on Transparent Conducting Substrates for Dye-Sensitized Solar Cells,” no. 9, pp. 3985–3990, 2009.